International Journal of Applied Pharmaceutics

ISSN- 0975-7058 Vol 16, Special Issue 1, 2024

Original Article

UNRAVELLING THE INTERACTION BETWEEN GARCINISIDONE-A AND HER2 PROTEIN IN BREAST CANCER: A COMPUTATIONAL STUDY

MAINAL FURQAN[1], DACHRIYANUS[2], MERI SUSANTI[3], PURNAWAN PONTANA PUTRA[4], FATMA SRI WAHYUNI[5*]

[1]Postgraduate Pharmacy Study Programme, Faculty of Pharmacy, Universitas Andalas, Padang-25163, Indonesia. [2,3]Faculty of Pharmacy, Universitas Andalas, Padang-25163, Indonesia. [4]Department of Pharmaceutical Chemistry, Faculty of Pharmacy, Universitas Andalas, Padang-25163, Indonesia. [5]Department of Pharmacology and Clinical Pharmacy, Faculty of Pharmacy, Universitas Andalas, Padang-25163, Indonesia

*Corresponding author: Fatma Sri Wahyuni; *Email: fatmasriwahyuni@phar.unand.ac.id

Received: 14 Oct 2023, Revised and Accepted: 23 Nov 2023

ABSTRACT

Objective: One substance found in the leaves of *Garcinia cowa* Roxb that has anticancer properties is garcinisidone-A. The study aims to simulate the docking of garcinisidone-A (Gar-A), molecular dynamics, and predict the ADME by predicting the binding of the HER2 protein in breast cancer cells and developing new drug candidate options for cancer treatment, often starting with computational analysis.

Methods: The research method involves computational utilization of pkCSM applications, Gar-A docking simulation with the HER2 protein using Gnina software version 1.0.2, and molecular dynamics conducted with GROMACS 2022.2 and CHARMMGUI applications.

Results: Gar-A has a molecular weight of less than 500, a Log P value of greater than 5, a limited amount of water solubility, a low level of skin permeability, good intestinal permeability, and a Convolutional Neural Network (CNN) pose score on the HER2 protein of 0.6178. It also does not readily cross the blood-brain barrier, and total clearance values indicate rapid elimination via other excretory routes or enzyme metabolism. Gar-A is thought to have interactions with HER2. There are hydrogen bond interactions with amino acids Lys753 and Asp863, carbon-hydrogen bonds with amino acids Leu785, Ser783, Thr862, and alkyl bonds with amino acids Leu726, Leu852, and Ile767. The stability of the Gar-A-substrate interaction could have been more evident during 100 ns molecular dynamics simulation.

Conclusion: The physicochemical properties of Gar-A align with Lipinski's rule for drug candidates. ADME predictions indicate good intestinal permeability for Gar-A; however, it suggests it cannot penetrate the blood-brain barrier. The docking results reveal that Gar-A has a value close to one which indicates similar action to its natural ligand and molecular dynamics simulations that Gar-A is less stable. The results illustrate that Gar-A has the potential as a breast anticancer.

Keywords: *Garcinia cowa*, ERBB2, Docking simulation, Molecular dynamics, ADME prediction

DOI: https://dx.doi.org/10.22159/ijap.2024.v16s1.24 Journal homepage: https://innovareacademics.in/journals/index.php/ijap

INTRODUCTION

Breast cancer is the most significant cause of death worldwide and the most common cancer in women. Globocan data show that in 2020, there were 65,858 new breast cancer cases out of 396,914 new cancer cases in Indonesia [1]. Breast cancer cells have a very high proliferation and differentiation ability due to cells expressing abnormal proteins or genes [2]. One of the most essential genes in breast cancer carcinogenesis is HER2 when overexpressed [3]. Research is conducted to obtain anticancer drugs by searching for natural compounds derived from plants such as *Garcinia cowa* Roxb, found in West Sumatra. Cytotoxic activity test research that has been carried out on this plant extract includes research on ethanol extract from *Garcinia cowa (G. cowa)* fruit peel, which has a cytotoxic effect on T47D breast cancer cells with an IC_{50} value of 19.33 µg/ml and ethanol extract of the bark also has a cytotoxic effect with an IC_{50} value of 5.10 µg/ml [4–6]. The dichloromethane fraction from fruit peel can induce apoptosis in cervical cancer cells tested on the HeLa cell line [7]. Compounds isolated from the bark of *G. cowa* include rubraxanthone, α-mangostin, and cowanin, all of which have strong cytotoxic activity *in vitro* against MCF-7 cells and H-460 cells [8]. The ethanol extract of *G. cowa* leaves provides a cytotoxic effect on T47D breast cancer cells with an IC_{50} value of 6.13±3.51 µg/ml and has a strong antioxidant effect with a value of 41.36±1.25 µg/ml [9, 10]. Compounds successfully isolated from Kandis tamarind leaves have been reported, namely methyl 2,4,6-trihydroxy-3-(3-methylbut-2-enyl)benzoate, garcinisidone-A (Gar-A) and 3-(1-methoxycarbonyl-4,6-dihydroxyphenoxy)-6-methoxy-3, 5-di(3-methyl-2-butenyl)-1,4-benzoquinone. Only Gar-A was active against H-460 lung cancer cells among the three isolated compounds, effective against MCF-7 breast cancer cells [11].

G. cowa exhibited the most potent leishmanicidal activity. To comprehend the interaction between phytochemicals derived from *G. cowa* (including cowanin, cowanol, cowaxanthone, norcowanin, rubraxanthone, and basic xanthones) and enzymes within the Leishmania donovani parasite, an *in silico* study was conducted, employing molecular docking analysis. The outcomes underscored the substantial potential of these phytochemicals as effective anti-leishmanial agents [12]. The anticancer activity of the gar-a compound can be tested *in silico* by utilising proteins available in the protein database (PDB).

An innovative trend in the development of pharmaceuticals is the use of computing in chemical research, which uses resources like big data, databases, and artificial intelligence (AI). This approach facilitates a quicker and more adequate understanding of compound properties in the quest for new drug candidates [13, 14]. Some examples of drugs that have gone through the *in silico* process are Captopril, Dorzolamide, Saquinavir, Rupintrivir, Oseltamivir, and Nevirapine [15-17]. Employing computational methods, particularly machine learning, to model the interaction between substances and biological targets offers a preliminary insight into toxicological effects, physicochemical characteristics, and possible drug targets [18]. In light of these advancements, to foresee how Gar-A will interact with proteins and bind to HER2, a study was done to forecast the drug's absorption, distribution, metabolism, excretion, docking simulation, and molecular dynamics.

The gap in research becomes apparent when it mentions that gar-a was effective against lung cancer cells, but its efficacy against breast cancer cells (MCF-7) needs further exploration. This sets the stage for the study that follows, which aims to investigate the anticancer activity of Gar-A on breast cancer cells and its interaction with the

HER2 protein using computational methods. In essence, the identified research gap revolves around the specific efficacy of Gar-A on breast cancer cells, necessitating a dedicated investigation to bridge this knowledge void and provide a more comprehensive understanding of its potential as an anticancer agent in the context of breast cancer.

MATERIALS AND METHODS

Absorption, distribution, metabolism, and excretion (ADME)

The pkCSM website was utilised for ADME prediction in the study, and the website link provided is https://biosig.lab.uq.edu.au/pkcsm/prediction [18]. Once access is secured, the compounds of interest are submitted in the subsequent step. On the pkCSM site, the chemical structure or information of the compounds can be submitted by users, and this submission method may include writing SMILES notation, uploading molecular files, or providing relevant details about the compounds. After the compounds are submitted, the pharmacokinetic properties, specifically the Absorption, Distribution, Metabolism, and Excretion (ADME) properties of the submitted compounds based on their chemical structures, are predicted by pkCSM. The results of these predictions, including numerical values and indicators detailing the ADME predictions for each compound, are generally categorised into absorption, distribution, metabolism, and excretion. The subsequent step involves the interpretation of the results obtained from pkCSM. Preparation for virtual screening is carried out using the data obtained from pkCSM. The data is prepared by considering the thresholds and criteria for ADME predictions.

Simulation of docking

The investigation for simulations utilised a Graphics Processing Unit (GPU) 1660 Super running CUDA version 11.6. The docking simulation process incorporated the HER2 target protein (PDB 3PP0), sourced from the Protein Data Bank website (https://www.rcsb.org). Identifying HER2 as one of the most crucial genes in breast cancer carcinogenesis when overexpressed [19] formed a crucial component in the investigation, guiding the selection of HER2 as the target for binding with the gar-a test compound. Gnina software version 1.0.2, with an Oriented docking system for the active site, was employed for the docking simulation, utilising Deep Learning as the assessment function [20]. The protein was separated from its natural ligand compound for preparation and a comparison ensued between the natural ligand from crystallography and the docking result. This step aimed to assess the Root Mean Square Deviation (RMSD) value, with a validation parameter set at RMSD score<2, signifying the similarity between the software's ability to simulate molecular docking and the results obtained through crystallography. Automatic generation of rectangular prisms occurred using CNN verbose software in Gnina, determining the maximum x, y, and z coordinates. The simulation employed a grid box with a completion set 64 and auto box ligands. Gar-A molecular geometry underwent improvement using tight binding from xTB version 6.0.4 [21]. The docking interaction between the protein and Gar-A was predicted using Discovery Studio version 2022.

Molecular dynamics

The molecular dynamics model simulation was conducted using Gromacs 2022.2 [22]. Initially, proteins were subjected to pre-treatment with CHARMMGUI. The first step involved access to the CHARMM-GUI website by opening a web browser and navigating to http://www.charmm-gui.org/. The force field Amber19Sb, with hydrogen mass partitioning [23, 24], was applied for a protein treatment. This process was streamlined by CHARMM-GUI, which automatically generated tailored input files for GROMACS. The GAFF2 force field was utilised for ligands [25, 26]. Following system preparation, the subsequent step was the downloading of GROMACS from the official website at http://www.gromacs.org/. After GROMACS was obtained, the software files were extracted, and environment variables on the computer were configured to set up the GROMACS environment. Returning to CHARMM-GUI, GROMACS-compatible topology and coordinate files were obtained for the computer system. These files served as the basis for creating GROMACS input files, including the molecular dynamics parameter file, topology file, and coordinate file. The OPC water model was used [27, 28]. In this research, minimization involved 50,000 steps with a maximum force set at less than 1000.0 kJ/mol/nm. With the input files in place, the subsequent steps involved energy minimization and equilibration. For equilibration, a canonical ensemble (NVT) with a Verlet scheme cutoff, a Coulomb-type Particle Mesh Ewald (PME), and a 100 ps step were employed [29]. Isothermal-isobaric equilibration (NPT) ensued using Parinello-Rahman pressure coupling, involving a stepwise equilibration of the system to achieve the desired temperature and pressure, running short MD simulations with position restraints on specific atoms [30]. A temperature of 310 K was maintained throughout the 100 nanoseconds of the production simulation, initiating the production MD run for the desired simulation time using GROMACS commands (gmx grompp and gmx mdrun). Once the simulation is complete, analyse the trajectory files generated during the MD run. Utilise GROMACS tools like gmx rms and gmx rmsf to extract information such as RMSD and RMSF, providing insights into the system's behaviour. All simulation parameters, results, and analyses were documented for future reference or publication, ensuring a comprehensive record of the entire simulation process [31].

Data analysis

Computational analysis, starting with the development of new medication options for the treatment of cancer, is frequently initiated by the pkCSM computational method. Proteins were simulated with Gnina software to simulate Gar-A, generating important physicochemical data about the compound and allowing for docking simulations to determine the best conformation. Further molecular dynamics simulations were conducted to assess the stability of both the test compound and protein.

RESULTS

The permeability is an important parameter in screening ligand-based drug similarity based on Lipinski's Rule of Five. The permeability is influenced by lipophilicity (log P), the number of hydrogen bond donors, hydrogen bond acceptors, and Molecular Weight (MW). Lipinski's Rules of Five provide criteria for evaluating the potential of a compound as a promising drug candidate. The thresholds are as follows: Log P should be less than 5, the number of hydrogen bond donors should be less than 5, the number of hydrogen bond acceptors should be less than 10, and the molecular weight should be less than 500 g/mol [32, 33]. The analysis of gar-a can be seen in table 1.

The binding energy value of Gar-A with HER2 was -7.56 kcal/mol. This indicates that the predicted binding of Gar-A with HER2 is an impulsive response anticipated to have a powerful interaction. The interaction of Gar-A with HER2 is in the form of hydrogen bonds with amino acids lysine and aspartic acid and forms carbon-hydrogen bonds with amino acids leucine, serine, threonine, pi sigma bonds with amino acid valine, pi alkyl bonds on leucine, isoleucine, alkyl bonds with amino acids alanine and leucine (fig. 1). The interaction between ligand and receptor is a pi-alkyl bond; this interaction occurs due to the interaction between aromatic and alkyl groups. The interaction occurs between amino acids Leu796 and Ala751. Pi-Sigma interaction is Val734. Alkyl-alkyl interactions are present in amino acids Leu726, Leu852, and Ile767. Hydrogen bond interactions with amino acids Lys733 and Asp863, and carbon-hydrogen bonds with amino acids Leu785, Ser783, and Thr 862.

Table 1: The physical and molecular characteristics of gar-a

No	Physical and chemical features	Data for gar-A	Rule of lipinski
1.	Weight in molecules	426.465	Less than 500 Da
2.	Log P	5.1543	Less than 5
3.	Bond that can be rotate	5	Not Available
4.	Acceptor of Protons	7	Less than 10
5.	Donor of protons	3	Less than 5
6.	Area of contact	180.368	Not Available

Table 2: ADME prediction of gar-A

No	Process	Data
1.	Absorption	
	Solubility in water	-3.68 (log. mol/l)
	P-glycoprotein substrate	Yes
	Absorption in the intestines	100 (%)
	Permeability of skin	-2.735 (log Kp)
	Permeability of Caco-2	-0.257 (log Papp in 10^{-6} cm/s)
2	Distribution	
	Volume of distribution	-0.001 (Log L/kg)
	Permeability of BBB	-1.268 (Log BB)
	Permeability of the CNS	-2.738 (Log PS)
3	Metabolism	
	CYP1-A2	No
	CYP2-C19	Yes
	CYP3-A4	Yes
4	Excretion	
	Clearance in total	0.322 (log ml/min/kg)

Table 3: Bond energy of the Gar-A with HER2 (3PP0) protein

PDB ID	Convolutional neural network score of pose	Affinity (kcal/mol)	Convolutional neural network affinity
3PP0	0.6178	-7.56	6.946

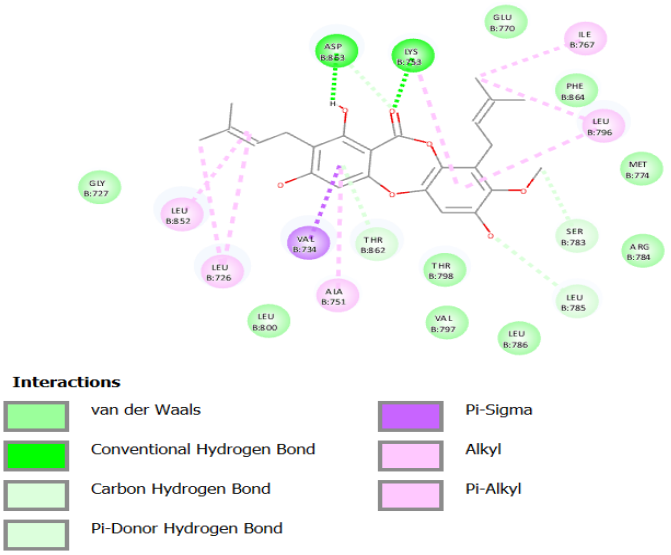

Fig. 1: Visualisation of the interaction between the HER2 protein and Gar-A (PDB ID; 3PP0)

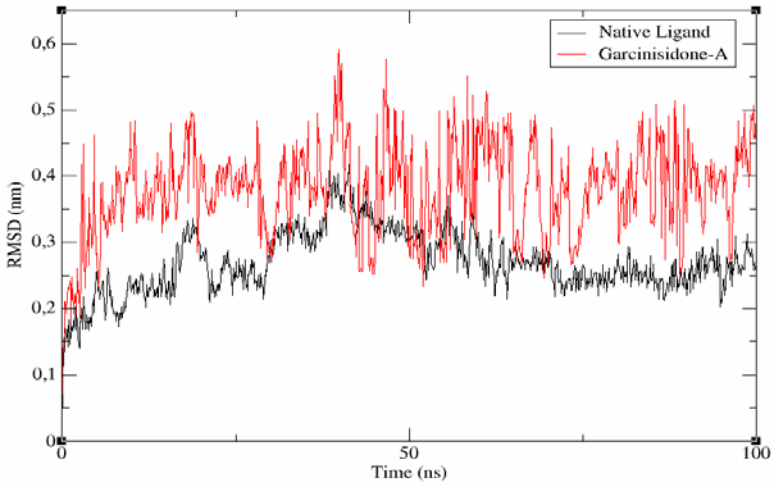

Fig. 2: RMSD results of native ligand and garcinisidone-a with simulation stability within 100 ns

In molecular dynamics simulations aimed at assessing the stability of Gar-A against HER2 protein over a total time of 100 ns, two key data points are typically obtained: RMSD (Root Mean Square Deviation) and RMSF (Root Mean Square Fluctuation). The stability analysis examines the RMSD plot, as shown in fig. 2, representing the complex formed between the natural ligand and the Gar-A complex throughout the 100 ns simulation. The analysis of RMSD plots for both complexes, the natural ligand and Gar-A indicates relatively lower stability in the formed complexes. The strength of the Gar-A and natural ligand complexes is achieved after the simulation exceeds 100 ns, with Gar-A fluctuating from 0.2 to 0.59 nm. Conversely, the natural ligand exhibits RMSD movements within the 0.2 to 0.4 nm range. Comparing these RMSD plot analyses with docking data describing the complex states between protein molecules and Gar-A during the simulation reveals that Gar-A experiences significant fluctuation in its RMSD values, suggesting dynamic interactions during the simulation process.

DISCUSSION

Based on previous research, it seems that various methods employ a diverse range of cancer cells. However, there has been no *in silico* research regarding the utilization of phytochemical compounds derived from *G. cowa* leaves, especially Gar-A. The relationship between Gar-A and HER2 protein in predicting absorption, distribution, metabolism, excretion, as well as docking and unexplored molecular dynamics for the development of promising new drug candidates in HER2-overexpressing breast cancer has not been investigated.

The log P value measures Gar-A hydrophobicity or lipophilicity, indicating how much it favours lipid environments. A higher log P value (>5) suggests increased hydrophobicity, potentially leading to an extended stay in lipid bilayers and wider distribution in the body. However, this extended stay in the bilayer can reduce the selectivity of binding to the target enzyme, potentially leading to higher toxicity. Conversely, excessively negative log P values may hinder the compound from passing through lipid bilayer membranes. However, it is crucial to note that this extended stay may reduce selectivity in binding to the target enzyme, possibly resulting in higher toxicity [32, 33].

The number of hydrogen bonds, both donors and acceptors, is crucial for a compound's biological activity, influencing the energy required for the absorption process. Higher bonding capacity requires more energy for the absorption process. Hydrogen bond donors provide hydrogen atoms for bond formation, while hydrogen bond acceptors receive hydrogen atoms to form bonds [34]. Gar-A, with limited solubility in water, can be absorbed by P-Glycoprotein. This protein plays a crucial role in substrate distribution to organs, indicating good intestinal permeability (log Papp>5 cm/s) [35].

Molecular weight has emerged as a significant factor influencing drug distribution. Compounds with molecular weights exceeding 500 g/mol may encounter challenges in efficiently crossing biological membranes, thereby impacting absorption kinetics and overall effectiveness. Consequently, the absorption of these drugs is likely to be prolonged, affecting their overall efficacy and absorption kinetics. It is a key consideration in drug design to optimise molecular weight for optimal membrane permeability and absorption rates. In contrast, compounds with smaller molecular weights will more easily penetrate biological membranes. The molecular weight of Gar-A being below 500, along with a log P>5, allows the prediction that Gar-A can be well-absorbed if given orally and meets one of the criteria for its potential as a drug candidate [36].

Gar-A has a low skin permeability, according to the skin permeation coefficient (log Kp) value of -2.735. The high permeability surface area product (log PS) and blood-brain barrier permeability (log BB) values show poorly distributed to the brain and unable to penetrate the CNS. The drug distribution process in the central nervous system relies on various factors, including blood flow to the brain, extracellular and intracellular fluid dynamics, pH conditions, low skin permeability, as well as values indicating poor distribution to the brain and inability to penetrate the CNS, indicate limited neurological impact [37]. Gar-A undergoes metabolism in the liver, mainly through the enzymes CYP2C19 and CYP3A4, with the CYP1A2 enzyme being the only one that does not metabolise it. Despite these metabolic pathways, the overall clearance value of 0.322 ml/min/kg indicates rapid elimination, possibly through other enzyme metabolism or alternative excretion pathways. Metabolic pathways, particularly via CYP2C19 and CYP3A4 enzymes, contribute to rapid elimination, reinforcing the need for further investigation into alternative excretion pathways [38].

Regarding its interaction with the HER2 protein, the docking result indicates a negative binding energy. The negative binding energy implies spontaneous binding, as outlined in table 3. The critical energy value reflects the affinity of Gar-A to the target protein, with a more negative value indicating a more stable bond between Gar-A and the protein. Furthermore, the pose score required for molecular dynamics simulation is close to one, indicating a similarity in action to the natural ligand. This alignment in pose score supports the findings from the docking process and suggests that Gar-A exhibits a molecular interaction with HER2 protein akin to its natural ligand [39].

Molecular dynamics simulations reveal that Gar-A exhibits decreased stability when forming protein complexes over 100 nanoseconds. The instability of the molecular dynamics data is caused by less than optimal interaction energy between the compound and the receptor, as well as receptor conformational flux caused by the shape of the binding pocket not fitting properly. Limitations in modelling flexible molecular movements, inaccurate energy estimates for predicting attachment affinity, and complexities and limitations of scoring functions and docking techniques indicate potential areas for improvement and further investigation [40]. This study effectively establishes a connection between the research objectives and a detailed exploration of the molecular properties of Gar-A, highlighting its potential as a promising drug candidate for breast cancer with HER2 overexpression. It also acknowledges the inherent limitations in computational modelling and simulation.

CONCLUSION

The physicochemical properties of Gar-A align with Lipinski's rule for drug candidates. ADME predictions indicate good intestinal permeability for Gar-A; however, it suggests it cannot penetrate the blood-brain barrier. In the context of its interaction with the HER2 protein, the CNN pose score is 0.6178. This score and molecular dynamics simulation result over 100 ns indicate that Gar-A forms less stable complexes with the protein. The instability observed during the simulation suggests dynamic fluctuations in the interaction between Gar-A and HER2 proteins.

ACKNOWLEDGEMENT

The author appreciates the support, guidance, and financial assistance the Faculty of Pharmacy Universitas Andalas provides under contract number 115/E5/PG.02.00. PL/2023 and expresses gratitude to Universitas Andalas' LPPM for helping to complete this task.

FUNDING

Universitas Andalas funded this research.

AUTHORS CONTRIBUTIONS

Conceptualization, Fatma Sri Wahyuni, Mainal Furqan, and Purnawan Pontana Putra; writing-original draft preparation, Mainal Furqan, Purnawan Pontana Putra, and Fatma Sri Wahyuni; writing-review and editing, Dachriyanus and Meri Susanti. The published version of the manuscript has been read and approved by all authors.

CONFLICT OF INTERESTS

The authors have disclosed no conflicts of interest. The writers affirm that the work in this article is their own, and they agree to be held liable for any claims based on its content.

REFERENCES

1. Observatory GC. Cancer today. International Agency for Research on Cancer; 2023. Available from:

https://gco.fr:iarc/today/fact-sheets-populations. [Last accessed on 09 Sep 2023]

2. Welcsh PL, Owens KN, King MC. Expression of BRCA1 and BRCA2 cellular levels of BRCA1 and BRCA2 proteins increases as cells progress through G1, peak during the S phase, and remain elevated during the G2-M transition. BRCA1, BRCA2, RAD51, and BARD1 co-localize during the S phase. S G2 M. 2000;16(2):G1.
3. Kong X, Zhang K, Wang X, Yang X, Li Y, Zhai J. Mechanism of trastuzumab resistance caused by HER-2 mutation in breast carcinomas. Cancer Manag Res. 2019;11:5971-82. doi: 10.2147/CMAR.S194137, PMID 31308740.
4. Husni E, Nahari F, Wirasti Y, Wahyuni FS, Dachriyanus. Cytotoxicity study of ethanol extract of the stem bark of asam kandis (Garcinia cowa Roxb.) on T47D breast cancer cell line. Asian Pacific Journal of Tropical Biomedicine. 2015;5(3):249-52. doi: 10.1016/S2221-1691(15)30013-7.
5. Wahyuni FS, Sutma S, Aldi Y. Uji efek sitotoksik ekstrak etanol kulit buah asam kandis (*Garcinia cowa* Roxb.) terhadap sel kanker payudara T47D dengan metoda MTT (Microtetrazolium). J Sains Teknol Farmasi. 2011;16(2):209-15.
6. Susanti M, Pratama AR, Suryani MI, Suryati, Dachriyanus. Development and validation of TLC-densitometry method for quantification of tetraprenyltoluquinone in the stem bark hexane extract of Garcinia cowa roxb. Heliyon. 2022;8(9):e10437. doi: 10.1016/j.heliyon.2022.e10437, PMID 36091948.
7. Wahyuni FS, Febria S, Arisanty D. Apoptosis induction of cervical carcinoma HeLa cells line by dichloromethane fraction of the rinds of *Garcinia cowa* Roxb. Phcog J. 2017;9(4):475-8. doi: 10.5530/pj.2017.4.76.
8. Wahyuni FS, Shaari K, Stanislas J, Lajis NH, Hamidi D. Cytotoxic xanthones from the stem bark of *Garcinia cowa* roxb. J Chem Pharm. 2015;7(1):227-36.
9. Wahyuni FS, Triastuti DH, Arifin H. Cytotoxicity study of ethanol extract of the leaves of Asam Kandis (*Garcinia cowa* Roxb.) on T47D breast cancer cell line. Phcog J. 2015;7(6):369-71. doi: 10.5530/pj.2015.6.9.
10. Jhofi M, Husni E, Hamidi D. Anticancer and antioxidant activity of Asam Kandis (*Garcinia cowa* Roxb) leaf extract and fraction. Advances in Health Sciences Research. 2nd International Conference on Contemporary Science and Clinical Pharmacy; 2021 Nov 17. p. 214-21. doi: 10.2991/ahsr.k.211105.032.
11. Wahyuni FS, Shaari K, Stanslas J, Lajis N, Hamidi D. Cytotoxic compounds from the leaves of *Garcinia cowa* Roxb. J App Pharm Sci. 2015 Feb 27;5(2):6-11. doi: 10.7324/JAPS.2015.50202.
12. Pyne N, Paul S. Screening of medicinal plants unraveled the leishmanicidal credibility of Garcinia cowa; highlighting norcowanin, a novel anti-leishmanial phytochemical through in-silico study. J Parasit Dis. 2022;46(1):202-14. doi: 10.1007/s12639-021-01441-7, PMID 35299910.
13. Mak KK, Pichika MR. Artificial intelligence in drug development: present status and future prospects. Drug Discov Today. 2019;24(3):773-80. doi: 10.1016/j.drudis.2018.11.014, PMID 30472429.
14. Zhavoronkov A, Vanhaelen Q, Oprea TI. Will artificial intelligence for drug discovery impact clinical pharmacology? Clin Pharmacol Ther. 2020;107(4):780-5. doi: 10.1002/cpt.1795, PMID 31957003.
15. Talele TT, Khedkar SA, Rigby AC. Successful applications of computer-aided drug discovery: moving drugs from concept to the clinic. Curr Top Med Chem. 2010;10(1):127-41. doi: 10.2174/156802610790232251, PMID 19929824.
16. Sliwoski GR, Meiler J, Lowe EW. Computational methods in drug discovery prediction of protein structure and ensembles from limited experimental data View project antibody modelling, antibody design, and antigen-antibody interactions view project. Comp Methods Drug Discov. 2014;66(1):334-95.
17. An J, Lee DCW, Law AHY, Yang CLH, Poon LLM, Lau ASY. A novel small-molecule inhibitor of the avian influenza H5N1 virus determined through computational screening against the neuraminidase. J Med Chem. 2009;52(9):2667-72. doi: 10.1021/jm800455g, PMID 19419201.
18. Pires DEV, Blundell TL, Ascher DB. pkCSM: predicting small-molecule pharmacokinetic and toxicity properties using graph-based signatures. J Med Chem. 2015;58(9):4066-72. doi: 10.1021/acs.jmedchem.5b00104, PMID 25860834.
19. Zhang ZM, Liu S, Lin K, Luo Y, Perry JJ, Wang Y. Crystal structure of human DNA methyltransferase 1. J Mol Biol. 2015;427(15):2520-31. doi: 10.1016/j.jmb.2015.06.001, PMID 26070743.
20. McNutt AT, Francoeur P, Aggarwal R, Masuda T, Meli R, Ragoza M. GNINA 1.0: molecular docking with deep learning. J Cheminform. 2021;13(1):43. doi: 10.1186/s13321-021-00522-2, PMID 34108002.
21. Bannwarth C, Ehlert S, Grimme S. GFN2-xTB-an accurate and broadly parametrized self-consistent tight-binding quantum chemical method with multipole electrostatics and density-dependent dispersion contributions. J Chem Theory Comput. 2019;15(3):1652-71. doi: 10.1021/acs.jctc.8b01176, PMID 30741547.
22. Abraham MJ, Murtola T, Schulz R, Pall S, Smith JC, Hess B. Gromacs: high-performance molecular simulations through multi-level parallelism from laptops to supercomputers. Software X. 2015;1-2:19-25. doi: 10.1016/j.softx.2015.06.001.
23. Gao Y, Lee J, Smith IPS, Lee H, Kim S, Qi Y. Charmm-gui supports hydrogen mass repartitioning and different protonation states of phosphates in lipopolysaccharides. J Chem Inf Model. 2021;61(2):831-9. doi: 10.1021/acs.jcim.0c01360, PMID 33442985.
24. Tian C, Kasavajhala K, Belfon KAA, Raguette L, Huang H, Migues AN. Ff19SB: amino-acid-specific protein backbone parameters trained against quantum mechanics energy surfaces in solution. J Chem Theory Comput. 2020;16(1):528-52. doi: 10.1021/acs.jctc.9b00591, PMID 31714766.
25. Sousa Da Silva AW, Vranken WF, ACPYPE-Ante Chamber P. Ython parser interface. BMC Res Notes. 2012;5:1-8.
26. Wang J, Wolf RM, Caldwell JW, Kollman PA, Case DA. 20035_Ftp. J Comp Chem. 2004;56531(9):1157-74.
27. Lee J, Hitzenberger M, Rieger M, Kern NR, Zacharias M, Im W. CHARMM-GUI supports the Amber force fields. J Chem Phys. 2020;153(3):035103. doi: 10.1063/5.0012280, PMID 32716185.
28. Mark P, Nilsson L. Structure and dynamics of the TIP3P, SPC, and SPC/E water models at 298 K. J Phys Chem A. 2001;105(43):9954-60. doi: 10.1021/jp003020w.
29. Darden T, York D, Pedersen L. Particle mesh Ewald: an N·log(N) method for Ewald sums in large systems. J Chem Phys. 1993;98(12):10089-92. doi: 10.1063/1.464397.
30. Parrinello M, Rahman A. Polymorphic transitions in single crystals: A new molecular dynamics method. J Appl Phys. 1981;52(12):7182-90. doi: 10.1063/1.328693.
31. Rahim F, Putra PP, Ismed F, Putra AE, Lucida H, Molecular Dynamics. Docking and prediction of absorption, distribution, metabolism, and excretion of lycopene as protein inhibitor of Bcl2 and DNMT1. Trop J Nat Prod Res. 2023;7(7):3439-44.
32. Lipinski CA. Lead and drug-like compounds: the rule-of-five revolution. Drug Discov Today Technol. 2004;1(4):337-41. doi: 10.1016/j.ddtec.2004.11.007, PMID 24981612.
33. Lipinski CA, Lombardo F, Dominy BW, Feeney PJ. Experimental and computational approaches to estimate solubility and permeability in drug discovery and development settings. Adv Drug Deliv Rev. 2001;46(1-3):3-26. doi: 10.1016/s0169-409x(00)00129-0, PMID 11259830.
34. Pajouhesh H, Lenz GR. Medicinal chemical properties of successful central nervous system drugs. Neurorx. 2005;2(4):541-53. doi: 10.1602/neurorx.2.4.541, PMID 16489364.
35. Dahlgren D, Lennernas H. Intestinal permeability and drug absorption: predictive experimental, computational and *in vivo* approaches. Pharmaceutics. 2019;11(8). doi: 10.3390/pharmaceutics11080411, PMID 31412551.
36. Agustina DW, Wahyuningsih MD, Widyarti S. Rifa'i M. Molecular docking study to reveal Morinda citrifolia fruits as a novel EGFR inhibitor for anticancer therapy. IOP Conf S Earth Environ Sci. 2021;743(1).
37. Bayat Z, Movaffagh J, Noruzi S. Development of a computational approach to predict blood-brain permeability on anti-viral

nucleoside analogues. Russ J Phys Chem. 2011;85(11):1923-30. doi: 10.1134/S0036024411110021.

38. Teo YL, Ho HK, Chan A. Metabolism-related pharmacokinetic drug-drug interactions with tyrosine kinase inhibitors: current understanding, challenges and recommendations. Br J Clin Pharmacol. 2015 Feb 1;79(2):241-53. doi: 10.1111/bcp.12496, PMID 25125025.
39. Halimi M, Bararpour P. Natural inhibitors of SARS-CoV-2 main protease: structure based pharmacophore modeling, molecular docking and molecular dynamic simulation studies. J Mol Model. 2022;28(9):279. doi: 10.1007/s00894-022-05286-6, PMID 36031629.
40. Pieroni M, Madeddu F, Di Martino J, Arcieri M, Parisi V, Bottoni P. MDligand–receptor: a high-performance computing tool for characterizing ligand-receptor binding interactions in molecular dynamics trajectories. Int J Mol Sci. 2023 Jul 1;24(14). doi: 10.3390/ijms241411671, PMID 37511429.